Bone 128 (2019) 115042

Contents lists available at ScienceDirect

Bone

journal homepage: www.elsevier.com/locate/bone

Full Length Article

Molecular profiling of failed endochondral ossification in mucopolysaccharidosis VII

Sun H. Peck[a,b], John W. Tobias[c], Eileen M. Shore[b,d], Neil R. Malhotra[a,b], Mark E. Haskins[e], Margret L. Casal[f], Lachlan J. Smith[a,b,*]

[a] Department of Neurosurgery, Perelman School of Medicine, University of Pennsylvania, 3450 Hamilton Walk, Philadelphia, PA, USA
[b] Department of Orthopaedic Surgery, Perelman School of Medicine, University of Pennsylvania, 3450 Hamilton Walk, Philadelphia, PA, USA
[c] Penn Genomic Analysis Core, University of Pennsylvania, 3620 Hamilton Walk, Philadelphia, PA, USA
[d] Department of Genetics, Perelman School of Medicine, University of Pennsylvania, 415 Curie Boulevard, Philadelphia, PA, USA
[e] Department of Pathobiology, School of Veterinary Medicine, University of Pennsylvania, 3800 Spruce St, Philadelphia, PA, USA
[f] Department of Clinical Sciences and Advanced Medicine, School of Veterinary Medicine, University of Pennsylvania, 3800 Spruce St, Philadelphia, PA, USA

ARTICLE INFO

Keywords:
Cartilage
Bone
RNA-Seq
Lysosomal diseases
Canine
Mucopolysaccharidosis
Sly Syndrome
Biomarkers

ABSTRACT

Mucopolysaccharidosis (MPS) VII is a lysosomal storage disorder characterized by deficient activity of β-glucuronidase, leading to progressive accumulation of incompletely degraded heparan, dermatan, and chondroitin sulfate glycosaminoglycans (GAGs). Patients with MPS VII exhibit progressive skeletal deformity including kyphoscoliosis and joint dysplasia, which decrease quality of life and increase mortality. Previously, using the naturally-occurring canine model, we demonstrated that one of the earliest skeletal abnormalities to manifest in MPS VII is failed initiation of secondary ossification in vertebrae and long bones at the requisite postnatal developmental stage. The objective of this study was to obtain global insights into the molecular mechanisms underlying this failed initiation of secondary ossification. Epiphyseal tissue was isolated postmortem from the vertebrae of control and MPS VII-affected dogs at 9 and 14 days-of-age (n = 5 for each group). Differences in global gene expression across this developmental window for both cohorts were measured using whole-transcriptome sequencing (RNA-Seq). Principal Component Analysis revealed clustering of samples within each group, indicating clear effects of both age and disease state. At 9 days-of-age, 1375 genes were significantly differentially expressed between MPS VII and control, and by 14 days-of-age, this increased to 4719 genes. A targeted analysis focused on signaling pathways important in the regulation of endochondral ossification was performed, and a subset of gene expression differences were validated using qPCR. Osteoactivin (*GPNMB*) was the top upregulated gene in MPS VII at both ages. In control samples, temporal changes in gene expression from 9 to 14 days-of-age were consistent with chondrocyte maturation, cartilage resorption, and osteogenesis. In MPS VII samples, however, elements of key osteogenic pathways such as Wnt/β-catenin and BMP signaling were not upregulated during this same developmental window suggesting that important bone formation pathways are not activated. In conclusion, this study represents an important step towards identifying therapeutic targets and biomarkers for bone disease in MPS VII patients during postnatal growth.

1. Introduction

The mucopolysaccharidoses (MPS) are a family of lysosomal storage diseases, where each subtype is characterized by mutations in one of the acid hydrolase genes responsible for the degradation of glycosaminoglycans (GAGs) [1]. These mutations result in production of encoded proteins with little or no activity, leading to the incomplete degradation and subsequent accumulation of GAG fragments. Progressive GAG accumulation results in cellular dysfunction and is associated with multi-systemic clinical manifestations, with patients exhibiting substantially diminished quality of life and shortened lifespan [2,3].

MPS VII (Sly Syndrome) is characterized by a mutation in the β-glucuronidase (*GUSB*) gene [4]. Impaired GUSB enzyme activity leads to progressive accumulation of aberrant degradation products of three types of GAGs: heparan, chondroitin, and dermatan sulfates [4]. Skeletal manifestations in MPS VII patients are severe [5–7]. In the spine, vertebral dysplasia and accelerated intervertebral disc degeneration lead to kyphoscoliosis and spinal cord compression resulting in related

* Corresponding author at: Department of Neurosurgery, University of Pennsylvania, 371 Stemmler Hall, 3450 Hamilton Walk, Philadelphia, PA 19104, USA.
E-mail address: lachlans@pennmedicine.upenn.edu (L.J. Smith).

https://doi.org/10.1016/j.bone.2019.115042
Received 22 April 2019; Received in revised form 14 August 2019; Accepted 19 August 2019
Available online 20 August 2019

neurological complications [5,6,8,9]. In joints, irregularities of the acetabula and femoral epiphyses have been reported in association with hip dysplasia [5], and restricted joint range of motion, contractures, and stiffness are common clinical observations [6]. Skeletal manifestations in MPS VII arise in part through impaired endochondral ossification of the vertebrae and long bones [8,10,11], which in normal postnatal development involves the ossification of a cartilaginous matrix that begins with a series of specified differentiation stages of resident cells [12,13]. In prior work using the naturally-occurring canine model, we showed that impaired endochondral ossification in MPS VII manifests in part as failed cartilage-to-bone conversion in secondary ossification centers during postnatal growth [11]. The resulting cartilaginous lesions (epiphyseal cartilage that fails to transition to bone) persist beyond skeletal maturity [14,15] and likely contribute to progressive spinal deformity and joint dysplasia. We also confirmed the presence of these lesions in a 19-year-old human MPS VII patient (the original patient of Dr. William Sly) [16] through post-mortem histological evaluation of vertebrae [8]. This patient exhibited progressive kyphoscoliotic deformity throughout postal growth. Delayed secondary ossification has also recently been demonstrated in MPS VII mice [16]. Collectively, these findings suggest that failures of endochondral ossification during postnatal growth are a common pathophysiological trait in both humans and animals with MPS VII. Further, persistent cartilaginous lesions have been described in MPS I dogs, suggesting failed endochondral ossification is common across different MPS subtypes [17]. Up until the recent approval of enzyme replacement therapy (ERT) for clinical use in 2017 [18], there were few treatment options for MPS VII patients. Laboratory and animal studies suggest ERT may at best have partial efficacy for treating skeletal abnormalities in MPS VII [9,19–23], highlighting the need for new approaches to specifically target and correct this debilitating aspect of the disease.

Endochondral ossification in both vertebrae and long bones begins with the condensation of mesenchymal progenitors. These cells differentiate into chondroblasts that undergo proliferation, followed by distinct stages of differentiation, which culminates in apoptosis followed by vascularization and osteoblast recruitment [13]. Chondrocyte differentiation occurs in primary and, later, secondary centers of ossification, and within the adjacent growth plates, enabling longitudinal bone growth. Differentiation stages include pre-hypertrophic, hypertrophic, and terminal, each characterized by expression of unique extracellular matrix (ECM) molecules, transcription factors, and receptors [13]. Previously, using post mortem microCT imaging and mRNA analyses, we identified the critical developmental window to be between 9 and 14 days-of-age when the vertebral and long bone epiphyses of unaffected dogs begin to ossify, but those of MPS VII dogs do not [10]. In this previous study, we also showed that the failure of endochondral ossification in MPS VII can be traced, in part, to the impaired ability of resident cells to undergo hypertrophic differentiation by measuring mRNA expression of epiphyseal chondrocyte differentiation markers across this developmental window [10].

Chondrocyte hypertrophic differentiation is regulated by a highly orchestrated pattern of signaling pathways, including fibroblast growth factors (FGFs), bone morphogenetic proteins (BMPs), Wingless/integrated (Wnts), Indian hedgehog (IHH), and others [24–28]. Together, these pathways form an inter-dependent signaling axis extending from the perichondrium to the growth plate, in which secreted growth factors tightly regulate the pace of chondrocyte proliferation and hypertrophic differentiation. We hypothesized that in MPS VII, impaired chondrocyte hypertrophic differentiation and subsequent lack of bone formation is associated with impaired activation and regulation of one or more of these signaling pathways, likely due to dysregulated distribution and availability of multiple signaling molecules as a result of aberrant GAG accumulation in the epiphyseal cartilage [29–32]. In this study, we used RNA-Seq to profile transcriptomic differences in epiphyseal tissue between MPS VII dogs and unaffected controls at both 9 and 14 days-of-age, in addition to temporal changes across this critical developmental window, with the goal of identifying the most dysregulated signaling pathways affecting chondrocyte differentiation and bone formation.

2. Materials and methods

2.1. Animals and tissue collection

For this study, we used the naturally-occurring canine model of MPS VII. MPS VII dogs have a missense mutation (R166H) in the GUSB gene [33] and exhibit a similar skeletal phenotype to human patients [8,14,33]. Animals were raised at the University of Pennsylvania School of Veterinary Medicine under NIH and USDA guidelines for the care and use of animals in research, and all studies were carried out with IACUC approval. Litter-matched control (heterozygous) and MPS VII (homozygous) dogs were identified via real time PCR analysis at birth. Animals (n = 5 for both control and MPS VII animals at each time point) were euthanized at 9 or 14 days-of-age, defined as number of postnatal days, using 80 mg/kg of sodium pentobarbital in accordance with the American Veterinary Medical Association guidelines. The thoracic spine was dissected out immediately following euthanasia, and epiphyseal tissue from both the cranial and caudal sides of the T12 vertebrae for each animal was excised adjacent to the growth plate (Fig. 1) with adjoining intervertebral disc tissue carefully removed. Cranial and caudal tissue for each sample was combined and flash frozen in liquid nitrogen. Microcomputed tomography (μCT) was used to verify the presence or absence of bone in secondary ossification centers for all samples using adjacent vertebrae (Fig. 1) (VivaCT40; Scanco Medical AG, Brüttisellen, Switzerland). Sequential axial images through the entire vertebra were obtained with an isotropic voxel size of 19 μm, an integration time of 380 ms, peak tube voltage of 70 kV, current of 0.114 mA, and an acquisition of 1000 projections per 180°. A three-dimensional Gaussian filter of 1.2 with a limited, finite filter support of 2 was used for noise suppression, and mineralized tissue was segmented from air or soft tissue using a threshold of 158. Bone formation was visualized through 3D μCT reconstructed images of the cartilaginous regions on the cranial and caudal ends of the primary ossification centers.

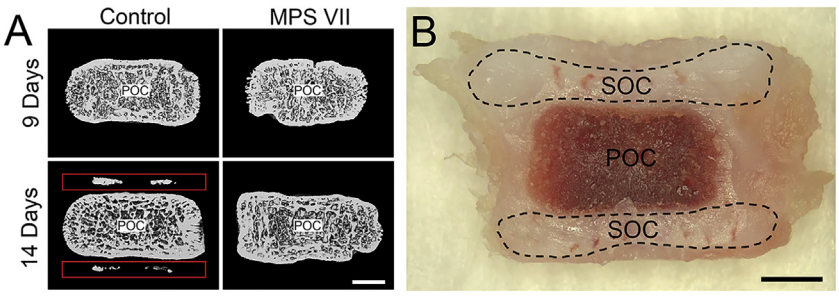

Fig. 1. A. Representative mid-coronal microcomputed tomography images of control and MPS VII thoracic dog vertebrae at 9 and 14 days-of-age, showing initial bone formation in the secondary ossification centers of 14 day-old controls, but no other groups. Red boxes indicate initial bone formation in the secondary ossification centers of 14-day old control animals. B. Gross, mid-coronal image of a thoracic, 9 day-old dog vertebra showing the regions of cranial and caudal epiphyseal tissue isolated via sharp dissection for RNA analysis. Scale = 2 mm. POC: primary ossification center; SOC: secondary ossification center. (For interpretation of the references to colour in this figure legend, the reader is referred to the web version of this article.)

2.2. RNA preparation and whole-transcriptome sequencing

Flash frozen epiphyseal tissue samples were pulverized using a mortar and pestle, and RNA was extracted using serial TRIzol (Ambion; Austin, TX)-chloroform extractions, with a modification to the standard protocol that we previously described for the RNA precipitation step to account for the high GAG content in cartilage that can co-precipitate with RNA [10]. Briefly, 100% isopropanol and a solution of 1.2 M NaCl and 0.8 M sodium citrate (Sigma-Aldrich; St. Louis, MO) in ddH_2O was used in a 1:1 mixture to separate contaminating GAGs from the RNA pellet. Following precipitation, extracted RNA was in-column treated with RNase-free DNase (Qiagen; Valencia, CA) on miRNeasy columns (Qiagen; Valencia, CA) and eluted following the manufacturer's protocols. The quality of each RNA sample was verified via BioAnalyzer using the Agilent RNA 6000 Pico Kit (Agilent; Santa Clara, CA) to ensure all samples used for library preparation had an RNA Integrity Number (RIN) value > 7. High quality total RNA from each sample was used to prepare RNA-Seq libraries using the TruSeq mRNA stranded kit (Illumina; San Diego, CA). Paired-end, 100-base pair sequencing was performed using the Illumina HiSeq 2500 platform with the results mapped to the canine genome version CanFam3.1 (NCBI) using Ensembl build 77. Pathway analysis was performed using Ingenuity Pathway Analysis (IPA; Qiagen, Valencia, CA, USA).

2.3. Validation of selected genes using qPCR

Real-time PCR validation of differential expression was performed for a panel of 11 genes (Supplementary Table 1), using the same RNA samples that were analyzed by RNA-Seq. For each sample, cDNA was synthesized from RNA isolated as described using SuperScript First-Strand Synthesis System for RT-PCR (Invitrogen; Carlsbad, CA). qPCR reactions were carried out on 10 ng of each cDNA sample per well using Fast SYBR Green Master Mix (Applied Biosystems; Foster City, CA) on a StepOnePlus Real-Time PCR system (Life Technologies; Carlsbad, CA). Primers were designed against *Canis familiaris* mRNA sequences published in the NCBI nucleotide database and are listed in Supplementary Table 1.

2.4. Statistical analyses

Differential gene expression between all groups from RNA-Seq results were determined using DESeq2 [34], with litter as a covariate and adjusted for false discovery rate to generate adjusted p-values, which are reported as p. Values of $p < 0.05$ were considered significant. For genes validated using qPCR, significant differences were established using 2-way analyses of variance (with age and disease state as the independent variables) with post-hoc Tukey's tests (Systat, Systat Software Inc.; San Jose, CA). Exact p-values were calculated to three decimal places and are presented as such, except for when $p < 0.001$, which are reported as $p < 0.001$. Results are expressed as mean ± standard deviation.

3. Results

3.1. Global analysis

Principal Component Analysis (PCA) of RNA-Seq data showed distinct clustering of each sample group, indicating clear effects of both age and disease state on global gene expression (Fig. 2A). Litter was included as a co-factor in the statistical analysis, but no significant effect of litter was found. At 9 days-of-age, 1375 genes were significantly differentially expressed between MPS VII and control, and by 14 days-of-age, this increased to 4719 genes (Fig. 2B). Examining temporal changes, for controls and MPS VII, 7514 and 4282 genes were significantly differentially expressed at 14 vs 9 days-of-age, respectively (Fig. 2B). The top significantly upregulated gene in MPS VII versus control was *GPNMB* (glycoprotein non metastatic melanoma B, or osteoactivin) at both 9 and 14 days-of-age (45 and 44-fold higher, respectively, both $p < 0.001$, Fig. 3A). The top significantly down regulated genes in MPS VII versus control were *ACP5* (tartrate resistant acid phosphatase, 8-fold lower, $p < 0.001$) and *WIF1* (Wnt Inhibitory Factor 1, 38-fold lower, $p < 0.001$) at 9 and 14 days-of-age, respectively (Fig. 3B).

3.2. Pathway analysis

Pathway analysis was performed using IPA, focusing on 15 pathways identified as having well-defined roles in the initiation and regulation of endochondral ossification (Fig. 4). At 9 days-of-age, 7 pathways, including hypoxia-inducible factor 1-alpha (HIF-1α), matrix metalloproteinases (MMPs), integrin signaling, osteoarthritis pathway, platelet-derived growth factor (PDGF) signaling, retinoic acid receptor (RAR) activation, and vascular endothelial growth factor (VEGF) signaling, exhibited overall significantly altered expression in MPS VII vs control. At 14 days-of-age, all 15 pathways exhibited overall significantly altered expression in MPS VII vs control (Fig. 4A). The matrix metalloproteinase (MMP) pathway exhibited the greatest percentage of significantly differentially expressed genes (MPS VII vs control) at both 9 and 14 days-of-age (30 and 48%, respectively, both $p < 0.001$). Examining temporal expression patterns, for controls, all 15 pathways exhibited significantly altered expression at 14 vs 9 days-of-age (Fig. 4B). For MPS VII, all but Hedgehog signaling, MMPs, and transforming growth factor-beta (TGF-β) signaling exhibited significantly altered expression at 14 vs 9 days-of-age, and the percent of significantly differentially expressed genes within these pathways at 14 vs 9 days-of-age was lower for MPS VII than for controls (Fig. 4B). A subset of significantly differentially expressed genes as identified by pathway analyses was validated via qPCR. Fold-changes were calculated from qPCR results and are presented in Supplementary Table 2.

3.3. Chondrocyte differentiation markers

We examined differential expression of selected markers of chondrocyte differentiation as a function of both disease state and age in our RNA-Seq dataset (Fig. 5). At 9 days-of-age, positive markers of chondrocyte maturation, including forkhead box protein A2 (*FOXA2*), myocyte enhancer factors 2C (*MEF2C*), *MMP13*, patched 1 (*PTCH1*), parathyroid hormone 1 receptor (*PTH1R*), and runt-related transcription factor 2 (*RUNX2*) were expressed at significantly lower levels in MPS VII vs control (Fig. 5A). At 14 days-of-age, in addition to these six genes, alkaline phosphatase (*ALPL*), osteocalcin (*BGLAP*), collagen type 10 A1 (*COL10A1*), and osteopontin (*SPP1*) were all significantly lower in MPS VII vs control. Expression of *SOX9*, a marker for chondrocyte proliferation that is downregulated as chondrocytes mature, was significantly higher in MPS VII vs control at 14 days-of-age. With respect to temporal changes in chondrocyte differentiation marker expression, in controls, positive markers of chondrocyte hypertrophy, including *ALPL*, *COL10A1*, *MEF2C*, *MMP13*, *RUNX2*, and *SPP1* were expressed at significantly higher levels at 14 vs 9 days-of-age, while negative markers aggrecan (*ACAN*), collagen type 2 A1 (*COL2A1*), and NK3 homeobox 2 (*NKX3-2*) were expressed at significantly lower levels (Fig. 5B). In MPS VII, the only positive markers of chondrocyte maturation to exhibit significantly higher expression at 14 vs 9 days-of-age were *MEF2C* and *RUNX2*, with the magnitude of the fold change less than for controls. Negative markers of chondrocyte maturation, *COL2A1* and *NKX3-2*, exhibited significantly lower expression in MPS VII at 14 vs 9 days-of-age, while *SOX9* exhibited significantly higher expression (Fig. 5B).

3.4. Matrix metalloproteinases

As noted above, the MMP pathway exhibited the greatest

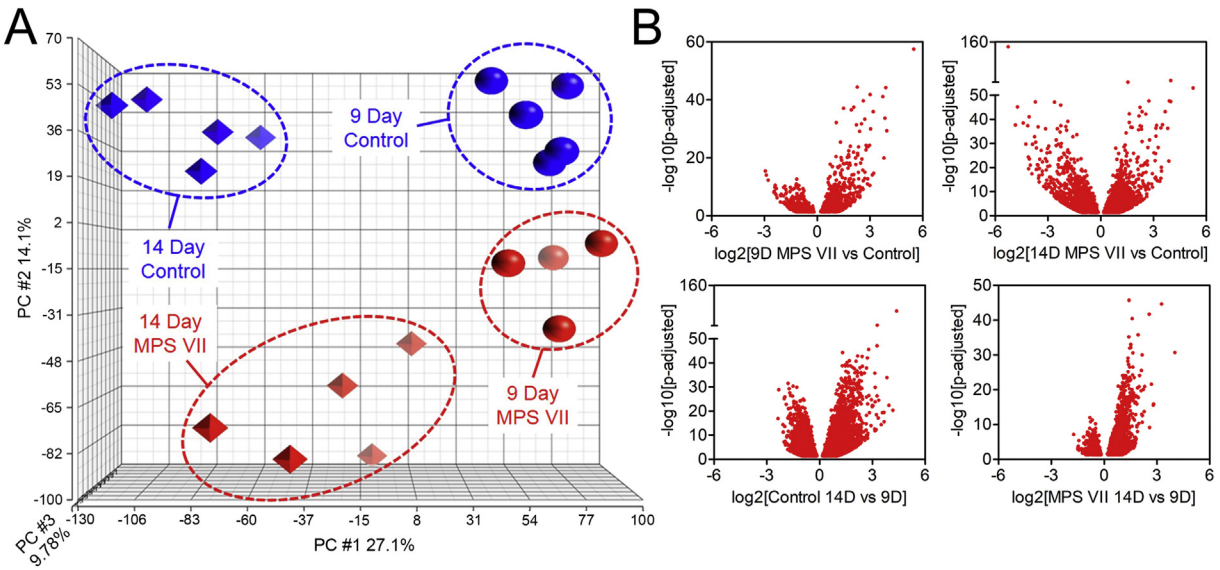

Fig. 2. A. Principal Component Analysis (PCA) of RNA-Seq data showing clustering of samples from each group, indicating clear effects of both disease state and age on global mRNA expression. B. Volcano plots illustrating relative numbers of genes significantly upregulated or downregulated as a function of disease state (MPS VII vs control, top) and age (14 vs 9 days-of-age, bottom).

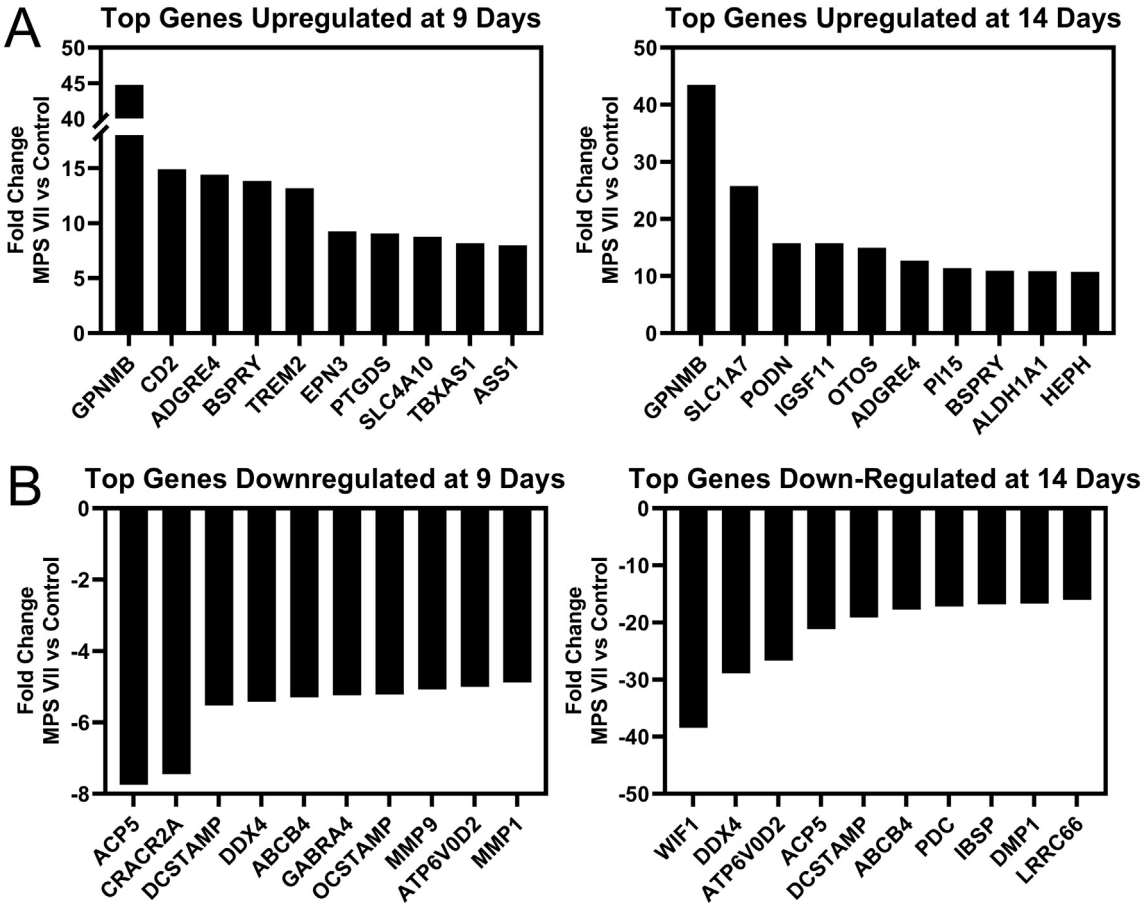

Fig. 3. A. Top 10 genes identified from RNA-Seq analysis as significantly upregulated in MPS VII epiphyseal tissue vs control at 9 (left) and 14 (right) days-of-age. B. Top 10 genes identified as significantly downregulated in MPS VII epiphyseal tissue vs control at 9 (left) and 14 (right) days-of-age.

percentage of significantly differentially expressed genes (MPS VII vs control) at both 9 and 14 days-of-age (Fig. 4A). MMPs are important for many biological processes involved in chondrocyte maturation and bone formation, including cartilage remodeling and angiogenesis [35]. At 9 days-of-age, MMPs and related inhibitors that were expressed at significantly lower levels in MPS VII vs control included *MMPs 1*, *3*, *9*, and *13*, and tissue inhibitor of metalloproteinase (*TIMPs*) *1* and *3*, while *MMPs 2*, *12*, *19* and *TIMP2* were expressed at significantly higher levels (Fig. 6A). At 14 days-of-age, in addition to the genes above, a disintegrin and metalloproteinases (*ADAMs*) *10*, *12* and *17*, *MMP14*, and

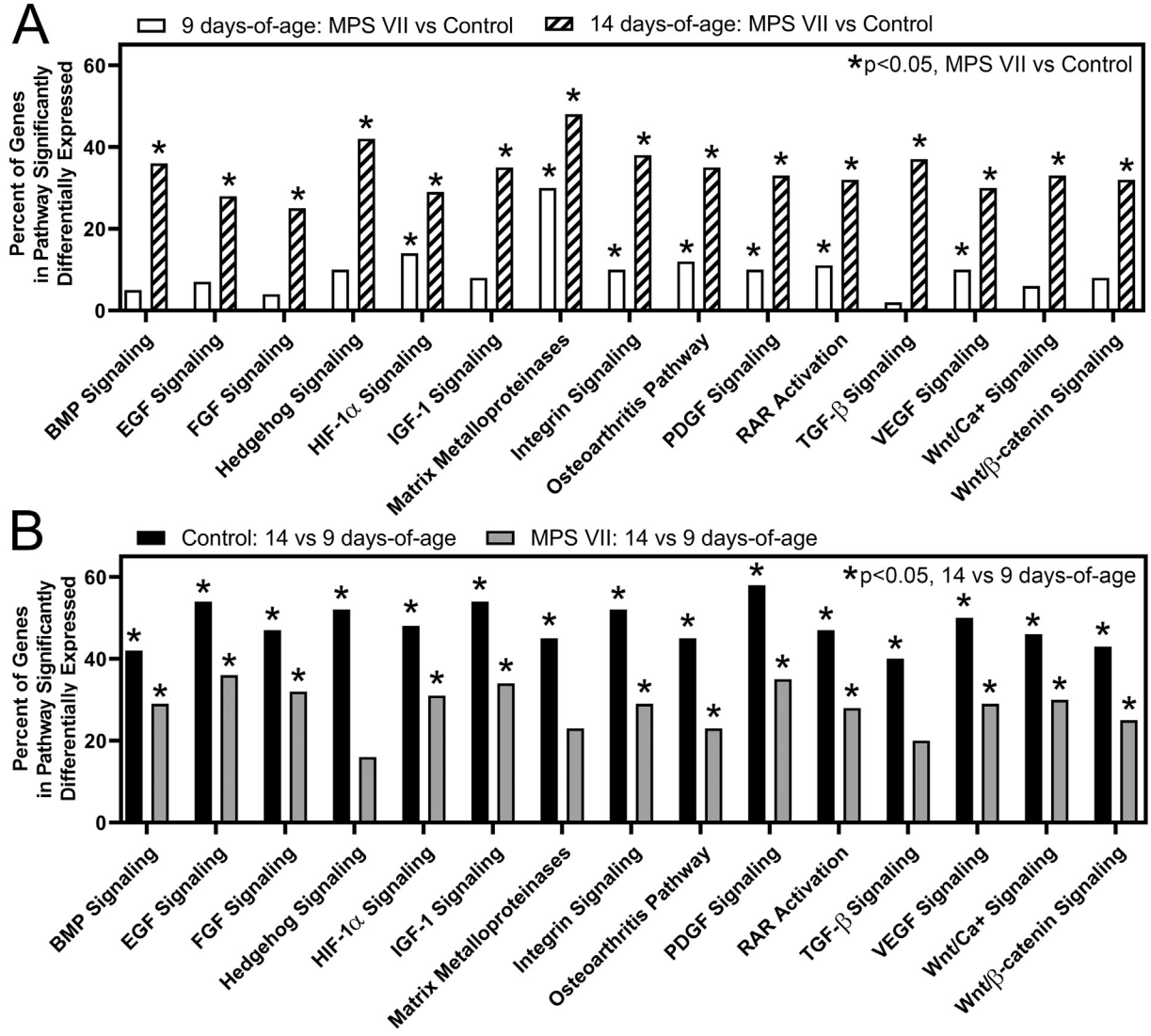

Fig. 4. Pathway analysis of RNA-Seq data for 15 pathways with established roles in the regulation of endochondral ossification, showing relative numbers of significantly differentially expressed genes within each pathway. A. Altered expression of endochondral ossification pathways as a function of disease state for epiphyseal tissue at 9 and 14 days-of-age. Asterisks indicate pathways that are significantly altered ($p < 0.05$, MPS VII vs control). B. Altered expression of endochondral ossification pathways as a function of age for control and MPS VII epiphyseal tissue. Asterisks indicate pathways that are significantly altered ($p < 0.05$, 14 vs 9 days-of-age).

tissue factor pathway inhibitor 2 (*TFPI2*) were expressed at significantly lower levels in MPS VII vs control. With respect to temporal changes, in controls, *ADAMs 10* and *17*, *MMPs 1*, *9*, *11*, *12*, *13*, and *TFIP2*, *TIMP1*, and *TIMP3* exhibited significantly higher expression at 14 vs 9 days-of-age, while *MMPs 2*, *16*, and *23B*, and *TIMP2* exhibited significantly lower expression (Fig. 6B). In MPS VII, *ADAMs 10* and *17*, *MMPs 12*, *13*, and *19* exhibited significantly higher expression at 14 vs 9 days-of-age, while *MMP2* and *TIMP1* exhibited significantly lower expression.

3.5. Wnt/β-catenin signaling

The Wnt/β-catenin signaling pathway, an essential positive regulator of chondrocyte hypertrophic differentiation and endochondral ossification [24–26,36], exhibited significantly altered overall expression as a function of both disease state and age (Fig. 4). Specifically, at 9 days-of-age, 8% of genes in this pathway exhibited significant differential expression (MPS VII vs control, $p = 0.127$, Fig. 4A), while at 14 days-of-age, this increased to 32% of pathway genes ($p < 0.001$). Notably, there was downregulation of both activating and inhibitory elements of Wnt/β-catenin signaling in MPS VII vs control, which was particularly evident at 14 days-of-age (Fig. 7A). Specific genes exhibiting significant differential expression at one or both ages included ligands (*WNTs 2B*, *3*, *4*, *5A*, and *9B*), inhibitors (dickkopf-related proteins (*DKKs*) 2 and 3, and *WIF1*), transcription factors (lymphoid enhancer-binding factor 1 (*LEF1*) and transcription factor 7 like 2 (*TCF7L2*)), receptors (frizzled (*FZD*) *1* and *5*), and other important regulatory elements (β-catenin (*CTNNB1*), dishevelled segment polarity proteins (*DVLs*) *1* and *2*, and glycogen synthase kinase 3 β (*GSK3B*)). With respect to temporal changes, for controls, 43% of genes in the Wnt/β-catenin pathway exhibited significant differential expression at 14 vs 9 days-of-age ($p < 0.001$, Fig. 4B), while for MPS VII, only 25% of genes in this pathway exhibited significant differential expression ($p = 0.001$).

3.6. BMP signaling

The BMP signaling pathway, another essential regulator of endochondral ossification [27], also exhibited significantly altered overall expression as a function of both disease state and age (Fig. 4). At 9 days-of-age, 5% of genes in this pathway exhibit significant differential

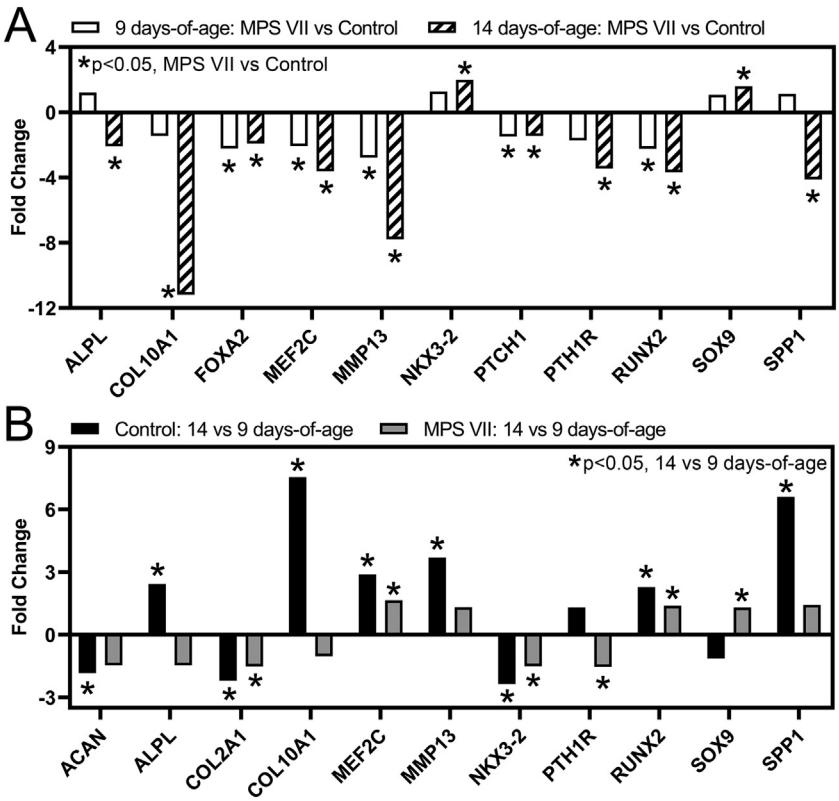

Fig. 5. Altered expression of selected chondrocyte differentiation markers in epiphyseal tissue from RNA-Seq analysis as a function of: A. Disease state (MPS VII vs control, at 9 and 14 days-of-age); and B. Age (14 vs 9 days-of-age, for control and MPS VII). Asterisks (*) indicate significant fold-changes in gene expression ($p < 0.05$).

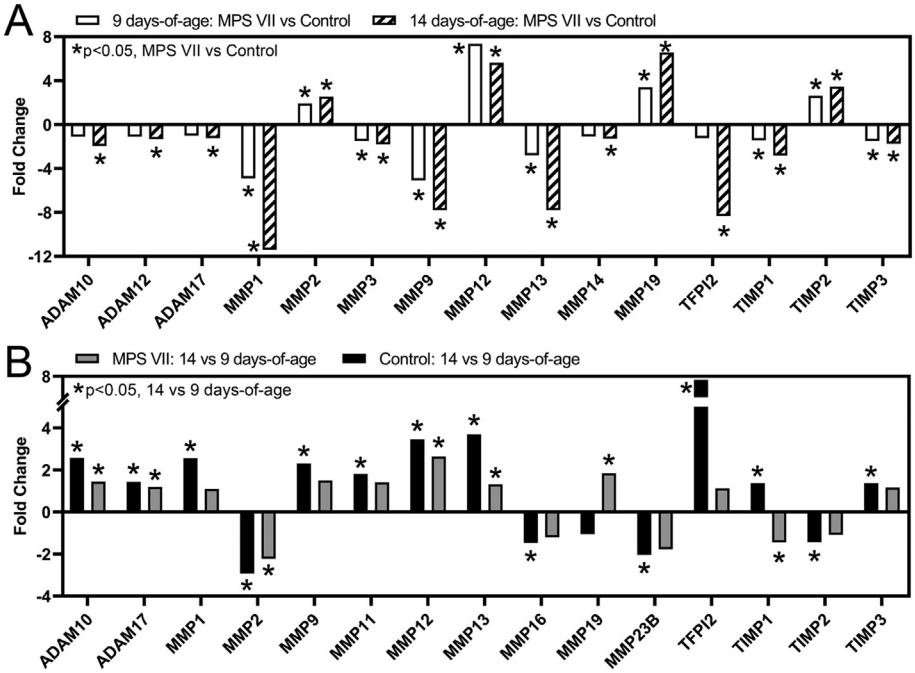

Fig. 6. Altered expression of selected matrix metalloproteinases and their inhibitors in epiphyseal tissue from RNA-Seq analysis as a function of: A. Disease state (MPS VII vs control, at 9 and 14 days-of-age); and B. Age (14 vs 9 days-of-age, for control and MPS VII). Asterisks (*) indicate significant fold-changes in gene expression ($p < 0.05$).

expression (MPS VII vs control, $p = 1.0$, Fig. 4A), while at 14 days-of-age, this increased to 36% of pathway genes ($p < 0.001$). With respect to specific genes (Fig. 8A), at 9 days-of-age, chordin (*CHRD*), a BMP inhibitor, was significantly upregulated in MPS VII vs control ($p < 0.001$). By 14 days-of-age, inhibitors *CHRD* and gremlin 1 (*GREM1*) were significantly upregulated in MPS VII vs control (both $p < 0.001$), while activating ligands BMPs 1, 2, and 4, and the co-factor Smad ubiquitin regulatory factor (E3 ubiquitin-protein ligase, *SMURF1*) were downregulated (all $p < 0.001$). With respect to temporal changes, in controls, there was significant upregulation of *BMPs 2*, *4*, and *8*, and follistatin (*FST*), and significant downregulation of *GREM1*, *CHRD*, and noggin (*NOG*) at 14 vs 9 days-of-age (Fig. 8B). In MPS VII, *BMP5*, *FST*, and *SMAD9* were significantly upregulated, and *BMPs 1* and *8B*, and *CHRD* significantly downregulated at 14 vs 9 days-of-age (all $p < 0.001$ except *CHRD*, $p = 0.045$).

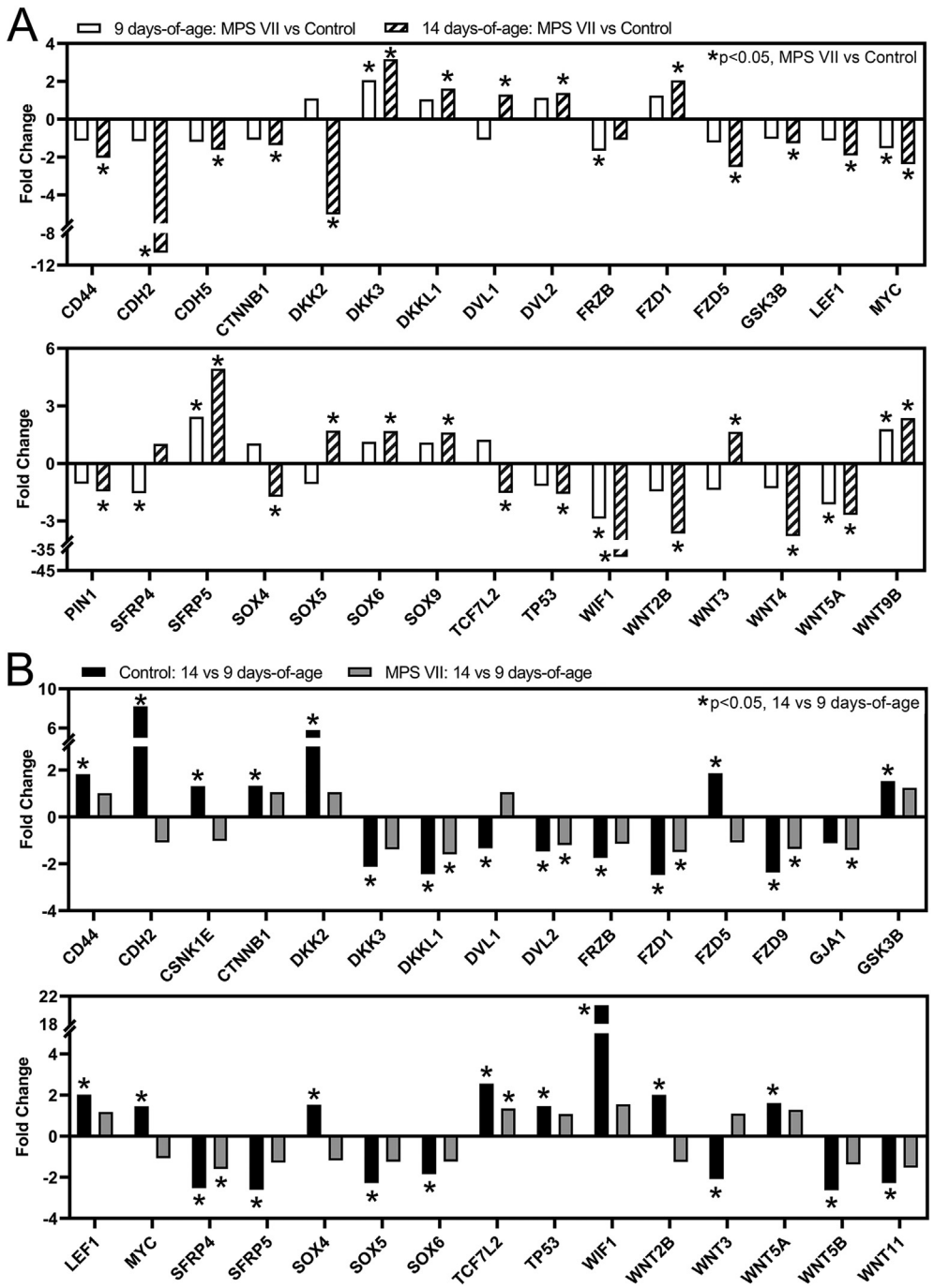

Fig. 7. Altered expression of selected Wnt/β-catenin signaling pathway genes in epiphyseal tissue from RNA-Seq analysis as a function of: A. Disease state (MPS VII vs control, at 9 and 14 days-of-age); and B. Age (14 vs 9 days-of-age, for control and MPS VII). Asterisks (*) indicate significant fold-changes in gene expression ($p < 0.05$).

4. Discussion

Patients with MPS suffer from debilitating skeletal abnormalities, including impaired bone formation through endochondral ossification during postnatal growth [19]. ERT was only recently approved for use in human MPS VII patients by the United States Food and Drug Administration (2017) and by the European Commission (2018) [18,37], and as of yet there is little published data on its efficacy specifically for bone disease. However, studies in MPS VII mice suggest that, similar to other MPS subtypes, ERT for MPS VII may at best be partially effective in this respect [23,23]. This is supported by the results of long term gene therapy studies in MPS VII dogs, in which despite very high levels of circulating enzyme, cartilaginous vertebral bone lesions persisted through the lifetime of the animals [15]. Therefore, there is a clinical need to develop therapies that specifically and effectively target bone manifestations in MPS VII patients.

Here, we used RNA-Seq to profile the transcriptome of epiphyseal tissue across the critical developmental window when secondary ossification fails to initiate in MPS VII dogs. Our previous work demonstrated that this failure is due in part to the impaired ability of resident epiphyseal chondrocytes to undergo hypertrophic differentiation [10]. The RNA-Seq results presented here confirm these findings, with chondrocytes in healthy controls exhibiting expected differential expression in upregulation of activators and downregulation of inhibitors

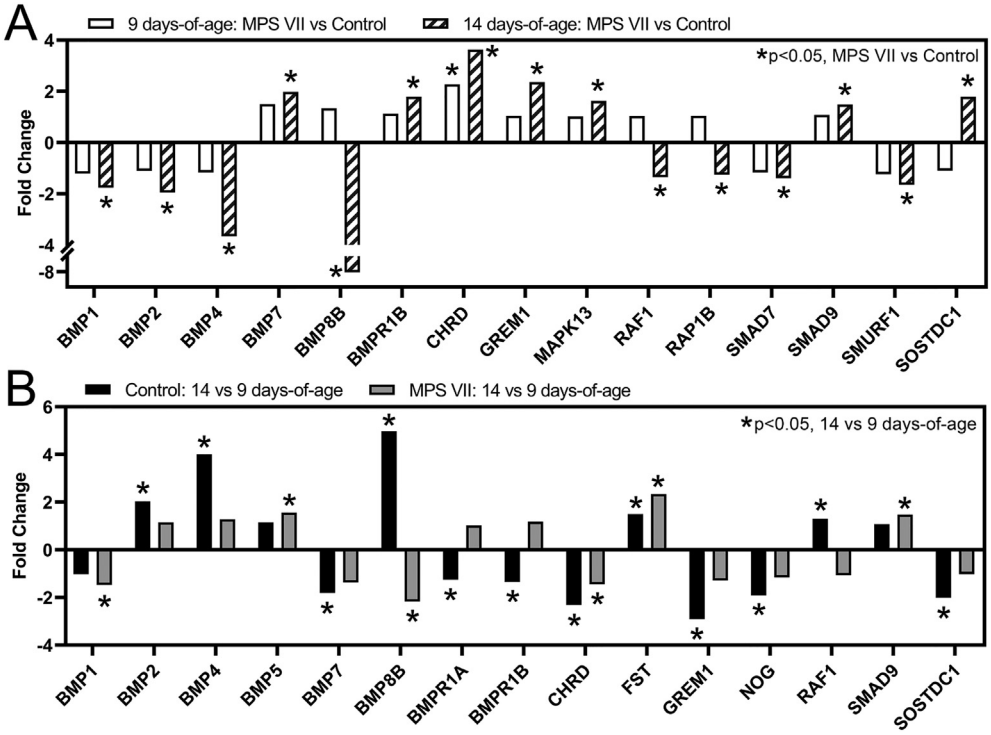

Fig. 8. Altered expression of selected BMP signaling pathway genes in epiphyseal tissue from RNA-Seq analysis as a function of: A. Disease state (MPS VII vs control, at 9 and 14 days-of-age); and B. Age (14 vs 9 days-of-age, for control and MPS VII). Asterisks (*) indicate significant fold-changes in gene expression ($p < 0.05$).

of hypertrophic maturation from 9 to 14 days-of-age, whereas similar differential expression and progression towards chondrocyte maturation are diminished or absent in MPS VII chondrocytes. Associated with this failure of hypertrophic differentiation, our results also demonstrated extensive dysregulation of the signaling pathways that regulate endochondral ossification. While the link between pathway dysregulation and the GAG accumulation that occurs in MPS VII has not been directly established, our previous work demonstrated that both intra and extracellular GAGs are elevated in MPS VII dog epiphyseal tissue at as early as 9 days-of-age and are likely contributing factors [10].

Matrix metalloproteinases are a major family of proteinases that play a critical role in ECM remodeling throughout the process of endochondral ossification. A finely-tuned balance between the expression of MMPs and their inhibitors must be maintained in both cartilaginous and mineralized tissues for bones to form normally [38,39]. Cartilage ECM resorption by MMP9 is a necessary step in endochondral ossification, in part by allowing growth factors such as VEGF access into the tissue for regulating angiogenesis, migration of additional growth factors and bone cells through newly formed vessels, and replacement with bone matrix [40]. Other MMPs, such as MMP13 and MMP14, play a role in remodeling the ECM during endochondral ossification when expressed by hypertrophic chondrocytes [41,42], as well as contributing to osteocyte perilacunar and pericanalicular remodeling, and directing bone cell migration and osteoblastic differentiation [42,43]. In our RNA-Seq data, the expression of MMPs 9, 13, and 14 were downregulated at 9 days-of-age in MPS VII animals compared to controls, and the magnitude of the fold-change of downregulation increased for all three genes at 14 days-of-age. Expression of ACP5 was also found to be significantly lower in MPS VII epiphyseal cartilage at the onset of secondary ossification. ACP5 encodes tartrate-specific acid phosphatase, an enzyme secreted by osteoclasts, chondroclasts and septoclasts that is essential for the degradation of mineralized matrix surrounding hypertrophic chondrocytes during the cartilage-to-bone transition [44]. Chondroclasts reside within cartilage canals [45], and lower expression of ACP5 is suggestive of reduced chondroclast numbers or activity, or that the cartilage canal network itself is diminished in MPS VII. Overall, diminished expression of these degradative enzymes in MPS VII epiphyseal cartilage suggests that the process of cartilaginous ECM removal is impaired, negatively impacting the necessary infiltration of vessels, cells, and growth factors needed for initiation of endochondral ossification.

Signaling pathways, such as Wnt/β-catenin and BMP, have broad roles in the regulation of endochondral ossification, including controlling the timing and pace of chondrocyte hypertrophic differentiation. While these regulatory roles have been most extensively studied in the context of the growth plate, the combination and sequence of signaling events that initiate chondrocyte hypertrophic differentiation within the cartilaginous secondary ossification centers is less well understood. Here, we show that both of these pathways exhibit significantly altered expression patterns from 9 to 14 days-of-age in vertebral secondary ossification centers, both for controls and MPS VII, although the magnitudes of pathway changes are markedly different between the two groups. In control dogs, this developmental window corresponds to the initiation of secondary ossification – at 9 days-of-age, only a cartilaginous template is present, and at 14 days, there is a small amount of mineralized bone (Fig. 1). In contrast, in MPS VII tissue, the cartilaginous template at 14 days-of-age is indistinguishable at the tissue level from 9 days. This suggests that in MPS VII, while some of the requisite mechanisms to initiate ossification may be occurring, they are insufficient to drive cellular and ECM changes at the rate occurring in controls. This may be due to a combination of factors, including signaling molecules being secreted at levels insufficient to initiate hypertrophy, those molecules being sequestered by GAGs accumulating in the ECM at abnormal levels, or cells being less able to respond to those molecules when they are presented. Providing the necessary signals exogenously has potential to normalize the timing and progression of bone formation in MPS VII.

With respect to the Wnt/β-catenin pathway in control animals, the transition from cartilage to bone was characterized by significant upregulation of downstream activating factors such as LEF1, CTNNB1, and TCF7L2, as well as inhibitors such as WIF1 and DKK2. It has been previously suggested that inhibitors such as WIF1 are expressed

concomitantly with Wnt activating elements in autoregulatory feedback loop during osteoblast maturation [46], and a similar mechanism may be present here. In MPS VII, the Wnt/β-catenin pathway gene expression changes from 9 to 14 days were diminished or absent, suggesting impaired pathway activation. With respect to the BMP pathway, the transition from cartilage to bone in controls was characterized by significant upregulation of secreted ligands classically associated with bone formation, including BMP2 and BMP4, with concomitant downregulation of inhibitors such as GREM1, NOG, and CHRD. Once again, in MPS VII, these changes in gene expression were largely absent from 9 to 14 days, consistent with impaired BMP pathway activity.

Therapeutic targeting of either or both of these pathways may be one strategy to normalize epiphyseal cartilage-to-bone conversion and subsequent bone formation in MPS VII. The potential limitations of ERT for addressing the bone manifestation in MPS are likely in part due to the inability of the very large enzyme to diffuse into poorly vascularized tissues such as epiphyseal cartilage. Administration of small molecules may be more effective than growth factors themselves, which, like endogenous molecules, may get sequestered by accumulated GAGs before reaching cells. Therefore, small molecules that stimulate osteogenic signaling and can be delivered in combination with ERT may have the greatest therapeutic efficacy. For example, GSK3B inhibitors, such as lithium, which function as indirect agonists of Wnt/β-catenin, have been shown to enhance bone formation in mice [47]. Similarly, small molecule agonists of canonical BMP signaling are currently under experimental evaluation [48,49]. The administration of osteogenic therapies could theoretically be limited and timed to coincide with key stages of skeletal development in MPS VII patients, with the goal of normalizing bone formation through to skeletal maturity. As these signaling pathways have broad regulatory roles that are not limited to the skeletal system, tissue-specific targeting may be important, particularly in children.

In addition to identifying new therapeutic targets, there is also a critical need for new disease-specific biomarkers that can be used for non-invasive monitoring of disease progression and response to therapy. Osteoactivin (glycoprotein non-metastatic melanoma B, *GPNMB*), an osteogenic factor shown to stimulate osteoblast differentiation [50], was found to be the top-ranked upregulated gene in MPS VII secondary ossification centers at both 9 and 14 days-of-age. Osteoactivin is a trans-membrane glycoprotein expressed by numerous cell types including various cancer cells, endothelial cells, macrophages, myocytes, chondrocytes, and all major bone cell types [51,52]. Osteoactivin has been shown to act as a positive regulator of osteoblast differentiation [53] and an inhibitor of osteoclast differentiation [54], and as such is being explored as a potential anabolic therapy for enhancing fracture healing [55]. Osteoactivin has also been linked to lysosomal dysfunction, potentially due to its role macroautophagy and phagocytosis [56], and its elevated expression has been linked to several lysosomal storage disorders where it has been proposed as a potential biomarker. In MPS VII, osteoactivin mRNA is upregulated in mouse aorta and brain [57,58]. In Gaucher disease, osteoactivin protein expression is elevated in serum, plasma, spleen, bone marrow, liver, and cerebral spinal fluid [59–61]; in Niemann-Pick Type C, protein is elevated in liver, spleen, and plasma [62]. Here, we provide evidence that osteoactivin may exhibit similar elevated expression in MPS VII skeletal tissue, and future work will examine its expression with age, across different tissues, and in response to therapeutic intervention to validate osteoactivin as a potential biomarker for MPS VII. Paradoxically, while osteoactivin can act as a positive regulator of bone formation, in this instance, its high expression in MPS VII epiphyseal cartilage, putatively as a consequence of lysosomal dysfunction, is associated with impaired chondrogenesis and endochondral ossification.

In this study, we used whole transcriptome sequencing to characterize the molecular events underlying failed initiation of secondary ossification in MPS VII dogs. We present an unbiased analysis of top dysregulated genes followed by a focused analysis centered around known regulators of endochondral ossification. While the results of this analysis are in some respects intuitive based on our previous work, they represent a logical first step towards identifying clinically relevant therapeutic targets. Future studies will assess additional pathways through similar focused analyses. A limitation of this work was the heterogeneous cellular composition of the samples analyzed, which is in general a limitation of all bulk RNA-Seq studies, and ongoing work is focused on examining spatial variations in expression of dysregulated molecules at the cellular level. Nonetheless our results identify key osteogenic pathways that fail to activate in MPS VII epiphyseal cartilage, preventing the cartilage-to-bone transition from occurring at the appropriate postnatal age. Such pathways represent potential therapeutic targets for normalizing bone formation in MPS VII dogs and patients.

Data availability statement

The datasets generated and analyzed during this study are available in the NCBI Gene Expression Omnibus (GEO) repository, accession number: GSE130088.

Acknowledgements

Funding for this work was received from the National Institutes of Health (R01AR071975, R01DK054481, R03AR065142, F32AR071298 and P40OD010939), the National MPS Society, and the Catharine D. Sharpe Foundation. Additional support was received from the Penn Center for Musculoskeletal Disorders (NIH P30AR069619). The authors thank the animal care staff at the University of Pennsylvania School of Veterinary Medicine for their support, and the staff of the Next Generation Sequencing Core for technical assistance with RNA-Seq experiments.

Author contributions

SHP contributed to conceptual design, performed experiments and data analysis, and drafted the manuscript; JWT performed biostatistical analyses; EMS and NRM provided conceptual input on experimental design; MEH and MLC cared for animals, assisted with post mortem tissue collection and provided conceptual input on experimental design; LJS contributed to conceptual design and data analysis, and drafted the manuscript. All authors reviewed and approved the manuscript prior to submission.

Appendix A. Supplementary data

Supplementary data to this article can be found online at https://doi.org/10.1016/j.bone.2019.115042.

References

[1] E.F. Neufeld, J. Muenzer, The mucopolysaccharidoses, in: C.R. Scriver, A.L. Beaudet, W.S. Sly, D. Valle (Eds.), The Metabolic and Molecular Bases of Inherited Disease, McGraw-Hill, New York, 2001, pp. 3421–3452.
[2] J. Muenzer, The mucopolysaccharidoses: a heterogeneous group of disorders with variable pediatric presentations, J Pediatr-US 144 (5) (2004) S27–S34.
[3] M. Stapleton, N. Arunkumar, F. Kubaski, R.W. Mason, O. Tadao, S. Tomatsu, Clinical presentation and diagnosis of mucopolysaccharidoses, Mol. Genet. Metab. 125 (1–2) (2018) 4–17.
[4] W.S. Sly, B.A. Quinton, W.H. Mcalister, D.L. Rimoin, Beta-glucuronidase deficiency - report of clinical, radiologic, and biochemical features of a new mucopolysaccharidosis, J Pediatr-US 82 (2) (1973) 249–257.
[5] R.D. Dekremer, I. Givogri, C.E. Argarana, E. Hliba, R. Conci, C.D. Boldini, A.P. Capra, Mucopolysaccharidosis type-vii (beta-glucuronidase deficiency) - a chronic variant with an oligosymptomatic severe skeletal dysplasia, Am. J. Med. Genet. 44 (2) (1992) 145–152.
[6] A.M. Montano, N. Lock-Hock, R.D. Steiner, B.H. Graham, M. Szlago, R. Greenstein, M. Pineda, A. Gonzalez-Meneses, M. Coker, D. Bartholomew, M.S. Sands, R. Wang, R. Giugliani, A. Macaya, G. Pastores, A.K. Ketko, F. Ezgu, A. Tanaka, L. Arash, M. Beck, R.E. Falk, K. Bhattacharya, J. Franco, K.K. White, G.A. Mitchell,

L. Cimbalistiene, M. Holtz, W.S. Sly, Clinical course of sly syndrome (mucopolysaccharidosis type VII), J. Med. Genet. 53 (6) (2016) 403–418.
[7] C. Vogler, B. Levy, J.W. Kyle, W.S. Sly, J. Williamson, M.P. Whyte, Mucopolysaccharidosis-vii - postmortem biochemical and pathological findings in a young-adult with beta-glucuronidase deficiency, Modern Pathol 7 (1) (1994) 132–137.
[8] L.J. Smith, G. Baldo, S. Wu, Y.L. Liu, M.P. Whyte, R. Giugliani, D.M. Elliott, M.E. Haskins, K.P. Ponder, Pathogenesis of lumbar spine disease in mucopolysaccharidosis VII, Mol. Genet. Metab. 107 (1–2) (2012) 153–160.
[9] S.H. Peck, M.L. Casal, N.R. Malhotra, C. Ficicioglu, L.J. Smith, Pathogenesis and treatment of spine disease in the mucopolysaccharidoses, Mol. Genet. Metab. 118 (4) (2016) 232–243.
[10] S.H. Peck, P.J.M. O'Donnell, J.L. Kang, N.R. Malhotra, G.R. Dodge, M. Pacifici, E.M. Shore, M.E. Haskins, L.J. Smith, Delayed hypertrophic differentiation of epiphyseal chondrocytes contributes to failed secondary ossification in mucopolysaccharidosis VII dogs, Mol. Genet. Metab. 116 (3) (2015) 195–203.
[11] L.J. Smith, J.T. Martin, S.E. Szczesny, K.P. Ponder, M.E. Haskins, D.M. Elliott, Altered lumbar spine structure, biochemistry, and biomechanical properties in a canine model of mucopolysaccharidosis type VII, J. Orthop. Res. 28 (5) (2010) 616–622.
[12] H.M. Kronenberg, Developmental regulation of the growth plate, Nature 423 (2003) 332–336.
[13] G. Karsenty, H.M. Kronenberg, C. Settembre, Genetic control of bone formation, Annu Rev Cell Dev Bi 25 (2009) 629–648.
[14] E.M. Xing, V.W. Knox, P.A. O'Donnell, T. Sikura, Y.L. Liu, S.S. Wu, M.L. Casal, M.E. Haskins, K.P. Ponder, The effect of neonatal gene therapy on skeletal manifestations in mucopolysaccharidosis VII dogs after a decade, Mol. Genet. Metab. 109 (2) (2013) 183–193.
[15] L.J. Smith, J.T. Martin, P. O'Donnell, P. Wang, D.M. Elliott, M.E. Haskins, K.P. Ponder, Effect of neonatal gene therapy on lumbar spine disease in mucopolysaccharidosis VII dogs, Mol. Genet. Metab. 107 (1–2) (2012) 145–152.
[16] Z.R. Jiang, A.L.K. Derrick-Roberts, M.R. Jackson, C. Rossouw, C.E. Pyragius, C. Xian, J. Fletcher, S. Byers, Delayed development of ossification centers in the tibia of prenatal and early postnatal MPS VII mice, Mol. Genet. Metab. 124 (2) (2018) 135–142.
[17] J.A. Chiaro, M.D. Baron, C.M. Del Alcazar, P. O'Donnell, E.M. Shore, D.M. Elliott, K.P. Ponder, M.E. Haskins, L.J. Smith, Postnatal progression of bone disease in the cervical spines of mucopolysaccharidosis I dogs, Bone 55 (1) (2013) 78–83.
[18] P. Harmatz, C.B. Whitley, R.Y. Wang, M. Bauer, W. Song, C. Haller, E. Kakkis, A novel blind start study design to investigate vestronidase alfa for mucopolysaccharidosis VII, an ultra-rare genetic disease, Mol. Genet. Metab. 123 (4) (2018) 488–494.
[19] N. Williams, D. Challoumas, D. Ketteridge, P.J. Cundy, D.M. Eastwood, The mucopolysaccharidoses: advances in medical care lead to challenges in orthopaedic surgical care, Bone Joint J 99b (9) (2017) 1132–1139.
[20] L.J. Smith, J.T. Martin, P. O'Donnell, P. Wang, D.M. Elliott, M.E. Haskins, K.P. Ponder, Effect of neonatal gene therapy on lumbar spine disease in mucopolysaccharidosis VII dogs, Molecular Genetics & Metabolism 107 (1–2) (2012) 145–152.
[21] D.J. Rowan, S. Tomatsu, J.H. Grubb, B. Haupt, A.M. Montano, H. Oikawa, C. Sosa, A. Chen, W.S. Sly, Long circulating enzyme replacement therapy rescues bone pathology in Mucopolysaccharidosis VII murine model, Molecular Genetics & Metabolism 107 (1–2) (2012) 161–172.
[22] C. Vogler, M.S. Sands, B. Levy, N. Galvin, E.H. Birkenmeier, W.S. Sly, Enzyme replacement with recombinant beta-glucuronidase in murine mucopolysaccharidosis type VII: impact of therapy during the first six weeks of life on subsequent lysosomal storage, growth, and survival, Pediatr. Res. 39 (6) (1996) 1050–1054.
[23] M.S. Sands, C. Vogler, J.W. Kyle, J.H. Grubb, B. Levy, N. Galvin, W.S. Sly, E.H. Birkenmeier, Enzyme replacement therapy for murine mucopolysaccharidosis type-Vii, J. Clin. Invest. 93 (6) (1994) 2324–2331.
[24] A.C. Andrade, O. Nilsson, K.M. Barnes, J. Baron, Wnt gene expression in the postnatal growth plate: regulation with chondrocyte differentiation, Bone 40 (5) (2007) 1361–1369.
[25] V. Church, T. Nohno, C. Linker, C. Marcelle, P. Francis-West, Wnt regulation of chondrocyte differentiation, J. Cell Sci. 115 (24) (2002) 4809–4818.
[26] X.Z. Guo, K.K. Mak, M.M. Taketo, Y.Z. Yang, The Wnt/beta-catenin pathway interacts differentially with PTHrP signaling to control chondrocyte hypertrophy and final maturation, PLoS One 4 (6) (2009).
[27] E. Minina, C. Kreschel, M.C. Naski, D.M. Ornitz, A. Vortkamp, Interaction of FGF, lhh/Pthlh, and BMP signaling integrates chondrocyte proliferation and hypertrophic differentiation, Dev. Cell 3 (3) (2002) 439–449.
[28] W.E. Samsa, X. Zhou, G. Zhou, Signaling pathways regulating cartilage growth plate formation and activity, Semin. Cell Dev. Biol. 62 (2017) 3–15.
[29] X.B. Ai, A.T. Do, O. Lozynska, M. Kusche-Gullberg, U. Lindahl, C.P. Emerson, QSulf1 remodels the 6-O sulfation states of cell surface heparan sulfate proteoglycans to promote Wnt signaling, J. Cell Biol. 162 (2) (2003) 341–351.
[30] S.K. Chintala, R.R. Miller, C.A. Mcdevitt, Role of heparan-sulfate in the terminal differentiation of growth-plate chondrocytes, Arch. Biochem. Biophys. 316 (1) (1995) 227–234.
[31] K. Jochmann, V. Bachvarova, A. Vortkamp, Heparan sulfate as a regulator of endochondral ossification and osteochondroma development, Matrix Biol. 34 (2014) 55–63.
[32] K.J. Manton, D.F.M. Leong, S.M. Cool, V. Nurcombe, Disruption of heparan and chondroitin sulfate signaling enhances mesenchymal stem cell-derived osteogenic differentiation via bone morphogenetic protein signaling pathways, Stem Cells 25 (11) (2007) 2845–2854.
[33] M.E. Haskins, R.J. Desnick, N. Diferrante, P.F. Jezyk, D.F. Patterson, Beta-glucuronidase deficiency in a dog - a model of human mucopolysaccharidosis-Vii, Pediatr. Res. 18 (10) (1984) 980–984.
[34] M.I. Love, W. Huber, S. Anders, Moderated estimation of fold change and dispersion for RNA-seq data with DESeq2, Genome Biol. 15 (12) (2014) 550.
[35] K. Yamamoto, H. Okano, W. Miyagawa, R. Visse, Y. Shitomi, S. Santamaria, J. Dudhia, L. Troeberg, D.K. Strickland, S. Hirohata, H. Nagase, MMP-13 is constitutively produced in human chondrocytes and co-endocytosed with ADAMTS-5 and TIMP-3 by the endocytic receptor LRP1, Matrix Biol. 56 (2016) 57–73.
[36] D.Y. Dao, J.H. Jonason, Y. Zhang, W. Hsu, D. Chen, M.J. Hilton, R.J. O'Keefe, Cartilage-specific beta-catenin signaling regulates chondrocyte maturation, generation of ossification centers, and perichondrial bone formation during skeletal development, J. Bone Miner. Res. 27 (8) (2012) 1680–1694.
[37] J.E. Fox, L. Volpe, J. Bullaro, E.D. Kakkis, W.S. Sly, First human treatment with investigational rhGUS enzyme replacement therapy in an advanced stage MPS VII patient, Mol. Genet. Metab. 114 (2) (2015) 203–208.
[38] K.B. Paiva, J.M. Granjeiro, Bone tissue remodeling and development: focus on matrix metalloproteinase functions, Archives of Biochemistry & Biophysics 561 (2014) 74–87.
[39] M. Prideaux, K.A. Staines, E.R. Jones, G.P. Riley, A.A. Pitsillides, C. Farquharson, MMP and TIMP temporal gene expression during osteocytogenesis, Gene Expr. Patterns 18 (1–2) (2015) 29–36.
[40] N. Ortega, K. Wang, N. Ferrara, Z. Werb, T.H. Vu, Complementary interplay between matrix metalloproteinase-9, vascular endothelial growth factor and osteoclast function drives endochondral bone formation, Dis. Model. Mech. 3 (3–4) (2010) 224–235.
[41] N. Johansson, U. Saarialho-Kere, K. Airola, R. Herva, L. Nissinen, J. Westermarck, E. Vuorio, J. Heino, V.M. Kahari, Collagenase-3 (MMP-13) is expressed by hypertrophic chondrocytes, periosteal cells, and osteoblasts during human fetal bone development, Dev. Dyn. 208 (3) (1997) 387–397.
[42] Y. Tang, R.G. Rowe, E.L. Botvinick, A. Kurup, A.J. Putnam, M. Seiki, V.M. Weaver, E.T. Keller, S. Goldstein, J. Dai, D. Begun, T. Saunders, S.J. Weiss, MT1-MMP-dependent control of skeletal stem cell commitment via a beta1-integrin/YAP/TAZ signaling axis, Dev. Cell 25 (4) (2013) 402–416.
[43] S. Barthelemi, J. Robinet, R. Garnotel, F. Antonicelli, E. Schittly, W. Hornebeck, S. Lorimier, Mechanical forces-induced human osteoblasts differentiation involves MMP-2/MMP-13/MT1-MMP proteolytic cascade, J. Cell. Biochem. 113 (3) (2012) 760–772.
[44] P.R. Odgren, H. Witwicka, P. Reyes-Gutierrez, The cast of clasts: catabolism and vascular invasion during bone growth, repair, and disease by osteoclasts, chondroclasts, and septoclasts, Connect. Tissue Res. 57 (3) (2016) 161–174.
[45] M.J. Blumer, S. Longato, E. Richter, M.T. Perez, K.Z. Konakci, H. Fritsch, The role of cartilage canals in endochondral and perichondral bone formation: are there similarities between these two processes? J. Anat. 206 (4) (2005) 359–372.
[46] B.L. Vaes, K.J. Dechering, E.P. van Someren, J.M. Hendriks, C.J. van de Ven, A. Feijen, C.L. Mummery, M.J. Reinders, W. Olijve, E.J. van Zoelen, W.T. Steegenga, Microarray analysis reveals expression regulation of Wnt antagonists in differentiating osteoblasts, Bone 36 (5) (2005) 803–811.
[47] P. Clement-Lacroix, M.R. Ai, F. Morvan, S. Roman-Roman, B. Vayssiere, C. Belleville, K. Estrera, M.L. Warman, R. Baron, G. Rawadi, Lrp5-independent activation of Wnt signaling by lithium chloride increases bone formation and bone mass in mice, P Natl Acad Sci USA 102 (48) (2005) 17406–17411.
[48] K. Vrijens, W.W. Lin, J. Cui, A. Shelat, M. Taylor, K.R. Guy, T.S. Chen, M.F. Roussel, Identification of small molecule agonists/activators of BMP-2, 4, 7 signaling, Cancer Res. (2011) 71.
[49] J.R. Genthe, J. Min, D.M. Farmer, A.A. Shelat, J.A. Grenet, W.W. Lin, D. Finkelstein, K. Vrijens, T.S. Chen, R.K. Guy, W.K. Clements, M.F. Roussel, Ventromorphins: a new class of small molecule activators of the canonical BMP signaling pathway, ACS Chem. Biol. 12 (9) (2017) 2436–2447.
[50] S.M. Abdelmagid, M.F. Barbe, M.C. Rico, S. Salihoglu, I. Arango-Hisijara, A.H. Selim, M.G. Anderson, T.A. Owen, S.N. Popoff, F.F. Safadi, Osteoactivin, an anabolic factor that regulates osteoblast differentiation and function, Exp. Cell Res. 314 (13) (2008) 2334–2351.
[51] C. Karlsson, T. Dehne, A. Lindahl, M. Brittberg, A. Pruss, M. Sittinger, J. Ringe, Genome-wide expression profiling reveals new candidate genes associated with osteoarthritis, Osteoarthr Cartilage 18 (4) (2010) 581–592.
[52] M. Singh, F. Del Carpio-Cano, J.Y. Belcher, K. Crawford, N. Frara, T.A. Owen, S.N. Popoff, F.F. Safadi, Functional roles of osteoactivin in normal and disease processes, Crit Rev Eukar Gene 20 (4) (2010) 341–357.
[53] N. Frara, S.M. Abdelmagid, G.R. Sondag, F.M. Moussa, V.R. Yingling, T.A. Owen, S.N. Popoff, M.F. Barbe, F.F. Safadi, Transgenic expression of osteoactivin/gpnmb enhances bone formation in vivo and osteoprogenitor differentiation ex vivo, J. Cell. Physiol. 231 (1) (2016) 72–83.
[54] G.R. Sondag, T.S. Mbimba, F.M. Moussa, K. Novak, B. Yu, F.A. Jaber, S.M. Abdelmagid, W.J. Geldenhuys, F.F. Safadi, Osteoactivin inhibition of osteoclastogenesis is mediated through CD44-ERK signaling, Exp. Mol. Med. 48 (2016).
[55] Y.Y. Huang, B. Bai, Y.C. Yao, Prospects of osteoactivin in tissue regeneration, Expert Opin Ther Tar 20 (11) (2016) 1357–1364.
[56] B. Li, A.P. Castano, T.E. Hudson, B.T. Nowlin, S.L. Lin, J.V. Bonventre, K.D. Swanson, J.S. Duffield, The melanoma-associated transmembrane glycoprotein Gpnmb controls trafficking of cellular debris for degradation and is essential for tissue repair, FASEB J. 24 (12) (2010) 4767–4781.
[57] G. Baldo, S.S. Wu, R.A. Howe, M. Ramamoothy, R.H. Knutsen, J.L. Fang, R.P. Mecham, Y.L. Liu, X.B. Wu, J.P. Atkinson, K.P. Ponder, Pathogenesis of aortic dilatation in mucopolysaccharidosis VII mice may involve complement activation, Mol. Genet. Metab. 104 (4) (2011) 608–619.

[58] M.K. Parente, R. Rozen, C.N. Cearley, J.H. Wolfe, Dysregulation of gene expression in a lysosomal storage disease varies between brain regions implicating unexpected mechanisms of neuropathology, PLoS One 7 (3) (2012).
[59] G. Kramer, W. Wegdam, W. Donker-Koopman, R. Ottenhoff, P. Gaspar, M. Verhoek, J. Nelson, T. Gabriel, W. Kallemeijn, R.G. Boot, J.D. Laman, J.P.C. Vissers, T. Cox, E. Pavlova, M.T. Moran, J.M. Aerts, M. van Eijk, Elevation of glycoprotein non-metastatic melanoma protein B in type 1 Gaucher disease patients and mouse models, Febs Open Bio 6 (9) (2016) 902–913.
[60] V. Murugesan, J. Liu, R.H. Yang, H.Q. Lin, A. Lischuk, G. Pastores, X.K. Zhang, W.L. Chuang, P.K. Mistry, Validating glycoprotein non-metastatic melanoma B (gpNMB, osteoactivin), a new biomarker of Gaucher disease, Blood Cell Mol. Dis. 68 (2018) 47–53.
[61] H. Zigdon, A. Savidor, Y. Levin, A. Meshcheriakova, R. Schiffmann, A.H. Futerman, Identification of a biomarker in cerebrospinal fluid for neuronopathic forms of Gaucher disease, PLoS One 10 (3) (2015).
[62] A.R.A. Marques, T.L. Gabriel, J. Aten, C.P.A.A. van Roomen, R. Ottenhoff, N. Claessen, P. Alfonso, P. Irun, P. Giraldo, J.M.F.G. Aerts, M. van Eijk, Gpnmb is a potential marker for the visceral pathology in Niemann-Pick type C disease, PLoS One 11 (1) (2016).